High Temp. Mater. Proc., Vol. **31** (2012), pp. 19–25 DOI 10.1515/HTMP.2011.124

Characterization of Alloys and Liquidus Projections of Ternary Bi-Sb-Sn system

Duško Minić,[1,*] Milan Kolarević,[2] Dragan Manasijević,[3] Vladan Ćosović,[4] Dragana Živković,[3] Nadežda Talijan[4] and Miljana Marković[1]

[1] University of Pristina, Faculty of Technical Sciences, Kosovska Mitrovica, Serbia

[2] University of Kragujevac, Machinery faculty, Kraljevo, Serbia

[3] University of Belgrade, Technical Faculty, Bor, Serbia

[4] University of Belgrade, Institute of Chemistry, Tehnology and Metallurgy, Belgrade, Serbia

Abstract. Given that Sn-based lead-free solders are considered as possible substitution for standard lead-tin solders, properties of the alloys from ternary Bi-Sb-Sn system were characterized by microstructural SEM-EDS analysis, Brinell hardness tests, and electrical conductivity measurements. Isothermal cross section at 298 K and liquidus surface projection were calculated by application of CALPHAD method and software package PANDAT 8.1. The experimentally determined phase compositions in analyzed microstructures were found to be in a good agreement with phases on calculated cross sections.

Keywords. Bi-Sb-Sn ternary system, hardness, electrical conductivity, isothermal sections, microstructure.

PACS®(2010). 81.05.Bx, 81.30.Bx, 81.70.Bt, 81.70.Ex, 68.37.Hk.

1 Introduction

The lead-tin alloy systems have been the most commonly used soldering materials in electronic interconnection and packaging due to their low cost and unique combination of physical, chemical and mechanical properties, good manufacturability and reliability. However, because of environmental and health concerns, the intensive research into finding alternative solder alloys is in progress.

* **Corresponding author:** Duško Minić, Faculty of Technical Sciences, Knjaza Milosa 7, 38220, Kosovska Mitrovica, Republic of Serbia; E-mail: dminic65@open.telekom.rs.

Received: July 11, 2011. Accepted: August 5, 2011.

Prior experimental study of two vertical sections, liquidus surface projection and isothermal section at room temperature of the ternary Bi-Sb-Sn system was carried out by Vogel and Apel [1] in the early 1950s. Liquidus surface projection that was defined at a time is presented in Figure 1. Three fields of primary crystallization are present and one invariant reaction of U-type takes place in the ternary system. Later study by Ghosh et al. [2], revealed existence of two invariant reactions of U-type. More recently, phase equilibria in the Bi-Sb-Sn ternary system have been studied experimentally and thermodynamically assessed by the calculation of phase diagram using CALPHAD method by Manasijevic et al. [3].

In this paper, we present isothermal section of ternary Bi-Sb-Sn system at 298 K, and liquidus surface projection calculated using CALPHAD method as well as mechanical properties i.e. Brinell hardness of 10 alloys of one vertical section and electrical conductivity of a larger number of alloys from three vertical sections which were used for calculation of isolines of electrical conductivity of entire Bi-Sb-Sn ternary system. Results of microstructural analysis of a number of (investigated) selected alloys are presented as well.

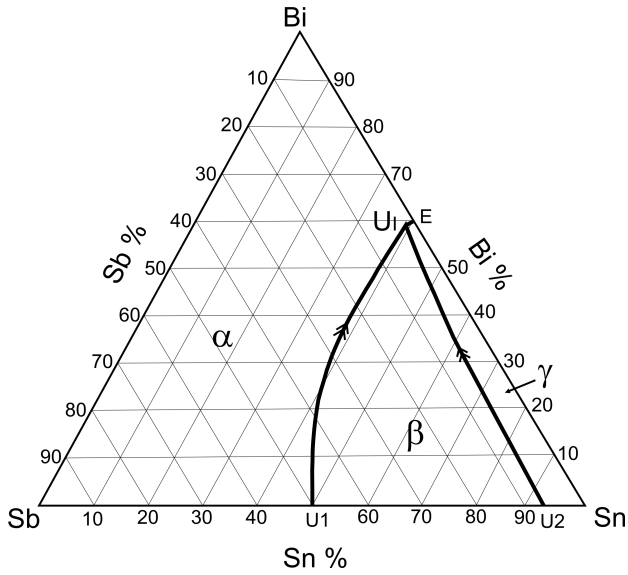

Figure 1. Liquidus surface projection [1].

2 Experimental Procedure

The alloy samples were prepared from high-purity (99.999 mass %) bismuth, antimony and tin powders produced by Alfa Aesar (Germany). The alloy samples weighting 4 g were prepared in inductive furnace under Argon atmosphere and subsequently cooled in air. The samples used for light microscopy, electrical conductivity measurements and hardness tests were prepared by classical metallographic procedure without etching, while the alloy samples used for SEM-EDS analysis were not sealed in polymer. Microstructural analysis was carried out by Scanning Electron Microscopy using JEOL (JSM6460) microscope equipped with Oxford Instruments Energy Dispersive Spectrometer and by light microscopy using OLYMPUS GX41 inverted metallographic microscope. Hardness of the selected samples was determined using HL-400DL impact hardness tester. Electrical conductivity measurements were carried out using Foerster SIGMATEST 2.069 eddy current instrument.

2.1 Thermodynamic Calculations

Thermodynamic data for the constitutive binary systems included in COST531 thermodynamic database [4] and CALPHAD method [5], were used for calculation of isothermal section of ternary Bi-Sb-Sn system at 298 K. Experimental thermodynamic data for the ternary Bi-Sb-Sn system were provided by Katayama et al. [6]. Phase common names, thermodynamic database names and Pearson's symbols [7] of the considered constitutive phases are listed in Table 1.

Phase common names	Thermodynamic database name	Pearson's symbol
L	LIQUID	–
(Bi), (Sb)	RHOMBO_A7	*hR*2
(Sn)	BCT_A5	*tI*4
β	SBSN	*cF*8
Sb_2Sn_3	SB2SN3	...

Table 1. Considered phases and their crystal structures [6].

3 Results and Discussion

3.1 Mechanical Properties

Hardness of the investigated alloys within the vertical BiSn-Sb section was determined using Brinell test method. Obtained values of hardness are presented on Figure 2.

Slight increase of hardness can be observed with the increase of antimony mole fraction from 0.3 to 0.5 as well as considerable increase of hardness for the alloys with the antimony mole fraction over 0.8.

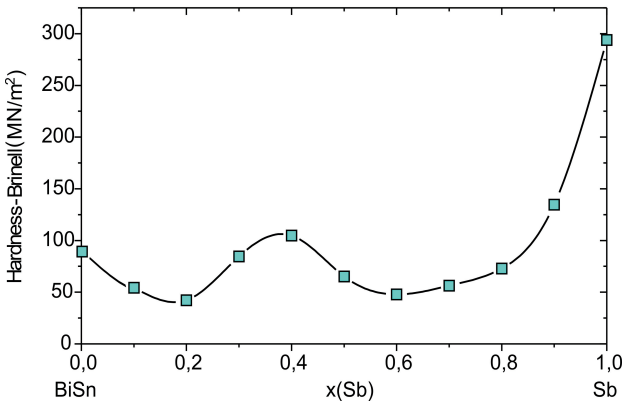

Figure 2. Hardness of alloys of ternary Bi-Sb-Sn system, vertical BiSn-Sb section.

3.2 Electrical Conductivity

Electrical conductivity (σ) of the ternary Bi-Sb-Sn system was investigated within three isothermal sections: BiSb-Sn, BiSn-Sb and SbSn-Bi. Compositions of the referring alloys and their electrical conductivities are given in Table 2. Graphical presentation of the relation between electrical conductivity and molar ratio of the alloys is presented on Figure 3.

BiSb-Sn		BiSn-Sb		SbSn-Bi	
x(Sn)	σ (MS/m)	x(Sb)	σ (MS/m)	x(Bi)	σ (MS/m)
0	0,865	0	0.653	0	0,996
0.1	1,078	0.1	0.822	0.1	1,357
0.2	0,926	0.2	1.853	0.2	0,955
0.3	0,895	0.3	1.005	0.3	0,786
0.4	0,923	0.4	2.164	0.4	0,854
0.5	0,968	0.5	1.573	0.5	0,756
0.6	1,132	0.6	1.817	0.6	0,703
0.7	1,327	0.7	1.384	0.7	0,462
0.8	1,648	0.8	1.551	0.8	0,396
0.9	3,647	0.9	2.202	0.9	0,639
1	8,695	1	2.5	1	0,769

Table 2. Alloy compositions and electrical conductivities.

Electrical conductivity of the alloys from the BiSn-Sb and BiSb-Sn sections exhibits moderate increase and rapid raise towards the pure metal corners. However, for the SbSn-Bi section it decreases up to 0.8 Bi mole fraction and then increases gently towards the Bi-rich corner.

Based on experimentally determined electrical conductivities of the alloys within the three quasi binary sections, electrical conductivity of ternary Bi-Sb-Sn system was determined by application of regression model [8]. Used theo-

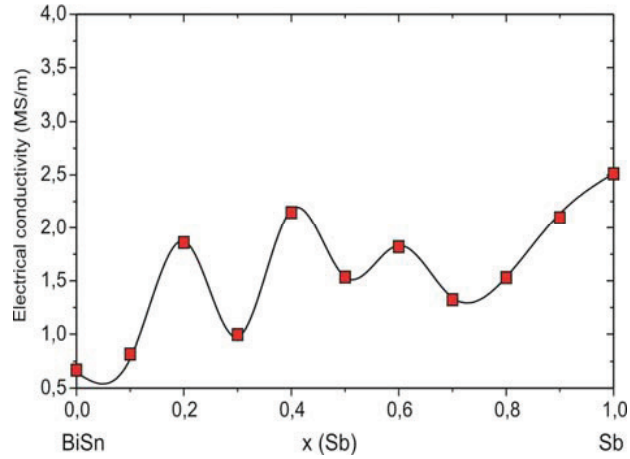

(a)

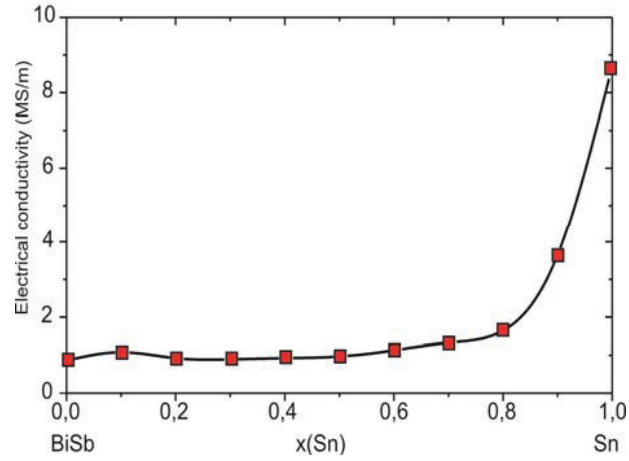

(b)

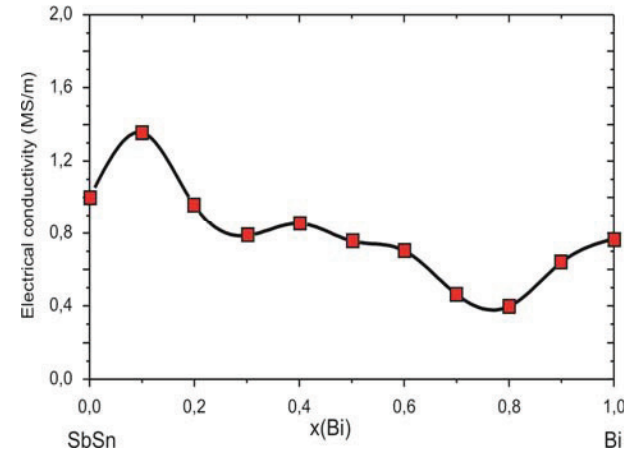

(c)

Figure 3. Electrical conductivity of ternary Bi-Sb-Sn system, (a) vertical BiSn-Sb section, (b) vertical BiSb-Sn section and (c) vertical SbSn-Bi section.

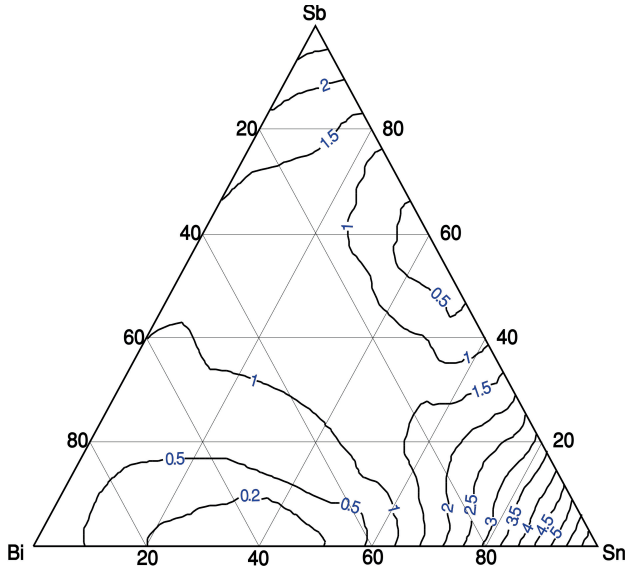

Figure 4. Isolines of electrical conductivity of the ternary Bi-Sb-Sn system.

retical regression model can be presented in a form of multiplied quasi linear regression:

$$\hat{Y} = b_1X_1 + b_2X_2 + b_3X_3 + b_{12}X_1X_2 + b_{13}X_1X_3 + b_{23}X_2X_3. \quad (1)$$

Unknown values of the coefficients of multiplied regression were determined by the least square method:

$$S = S(b_1, b_2, b_3, b_{12}, b_{13}, b_{23}) = \sum_{i=1}^{N} \varepsilon_i^2 = \sum_{i=1}^{N} (Y_i - \hat{Y}_i)^2 \quad (2)$$

$$S = \sum_{i=1}^{N} \varepsilon_i^2 = \sum_{i=1}^{N} \left[Y_i - (b_1X_1 + b_2X_2 + b_3X_3 + b_{12}X_1X_2 + b_{13}X_1X_3 + b_{23}X_2X_3)_i \right]^2. \quad (3)$$

The values of regression coefficients were determined, and used mathematical model, presented by Equation (1) can be written as:

$$\begin{aligned} \sigma(\mathrm{MS/m}) &= 5.1714 \times (\mathrm{Sn}) + 2.5303 \times (\mathrm{Sb}) \\ &+ 0.6155 \times (\mathrm{Bi}) - 10.1238 \times (\mathrm{Sn}) \times (\mathrm{Sb}) \\ &- 8.1498 \times (\mathrm{Sn}) \times (\mathrm{Bi}) + 0.9651 \times (\mathrm{Sb}) \times (\mathrm{Bi}). \end{aligned} \quad (4)$$

Graphical representation of the mathematical model defined by Equation (4) is given in Figure 4.

For quasi-linear model of multiplied regression given by Equation (1) the squares of discrepancies of empiric values from regression equation and sum of squares of discrepancies was obtained SK = 17.60867152. As the absolute

Sample	Sample composition (at. %)	Experimentally determined phases	Bi (at. %)		Sb (at. %)		Sn (at. %)	
			exp.	calc.	exp.	calc.	exp.	calc.
I	Bi = 41 Sb = 49.5 Sn = 9.5	(Sb) (Bi) β	6.24 93.45 4.72	4.72 95.69 1.67	92.64 4.23 52.36	94.5 4.27 57.07	1.12 2.32 42.92	0.78 0.04 41.26
II	Bi = 40 Sb = 19 Sn = 41	(Sn) (Bi) β	1.89 97.46 2.43	1.32 99.32 1.95	1.23 2.25 42.12	$8.5.10^{-5}$ 0.22 46.05	96.88 0.29 55.45	98.67 0.46 52
III	Bi = 6 Sb = 48 Sn = 46	(Sb) β	95.75 2.23	98.18 1.06	3.46 49.87	1.75 51.76	0.79 47.9	0.07 47.18
IV	Bi = 9.5 Sb = 30.5 Sn = 60	(Sn) (Bi) β	0.87 95.43 3.54	1.32 99.32 1.95	0.74 2.78 42.09	$8.5.10^{-5}$ 0.21 46.05	98.39 1.79 54.37	98.67 0.467 52

Table 3. Calculated and experimentally determined phase compositions in the ternary Bi-Sb-Sn system at 298 K.

value of the greatest discrepancies was $\varepsilon_{max} = 2.45926$ and less than 3*E = 2.683942518 so based on the three σ rule, the assumed functional dependence was considered accurate.

3.3 Isothermal Section at 298 K

Comparative presentation of the calculated and isothermal section of the ternary Bi-Sb-Sn system at 298 K from literature, are presented in Figure 5. Marked compositions correspond to the samples analyzed using light (□) and electron (◯) microscopy. Earlier studies [1] show that ternary system consists of three single-phase regions (α, β and γ), three two-phase regions ($\alpha + \beta$, $\alpha + \gamma$ and $\beta + \gamma$) and one three-phase region ($\alpha + \beta + \gamma$). Calculations, on the other side, suggest existence of eight regions in the isothermal section at 298 K, including two single-phase, four two-phase and two three-phase regions. Hence, on Figure 5, significant difference between calculated isothermal section and literature data can be observed. According to Ghosh et al. [2] the solid solubility of Sb in (Sn) reported by Vogel and Apel [1] at 298 K is considerably higher than that in presently accepted Sb-Sn phase diagram and moreover, vertical section reported at 30 wt. % is not consistent with the binary phase diagram. Therefore, observed differences could be attributed to all this inconsistencies.

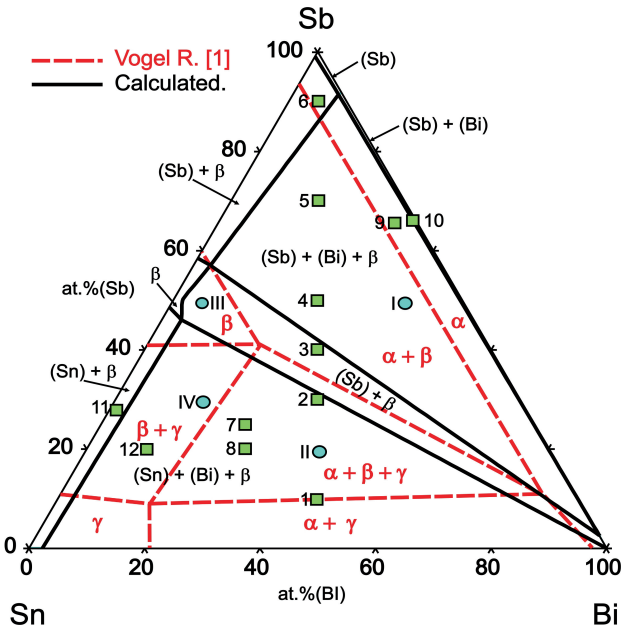

Figure 5. Comparative presentation of the calculated and isothermal section of the ternary Bi-Sb-Sn system at 298 K from literature [1].

Sample	Bi (at. %)	Sb (at. %)	Sn (at. %)
1	45	10	45
2	35	30	35
3	30	40	30
4	25	50	25
5	15	70	15
6	5	90	5
7	25	25	50
8	27	20	53
9	30	65	5
10	33,5	66	0,5
11	1	26	73
12	10	20	70

Table 4. Chemical composition of the investigated alloys.

Type	T (K)	Reaction	Bi (at.%)	Sb (at.%)	Sn (at.%)
U1	517,23	LIQUID + SB2SN3 → SBSN + BCT_A5	0,3646	8,8108	90,8246
U2	411,62	LIQUID + SBSN → RHOMBO_A7 + BCT_A5	37,5569	1,1221	61,321

Table 5. Invariant reactions of ternary Bi-Sb-Sn system.

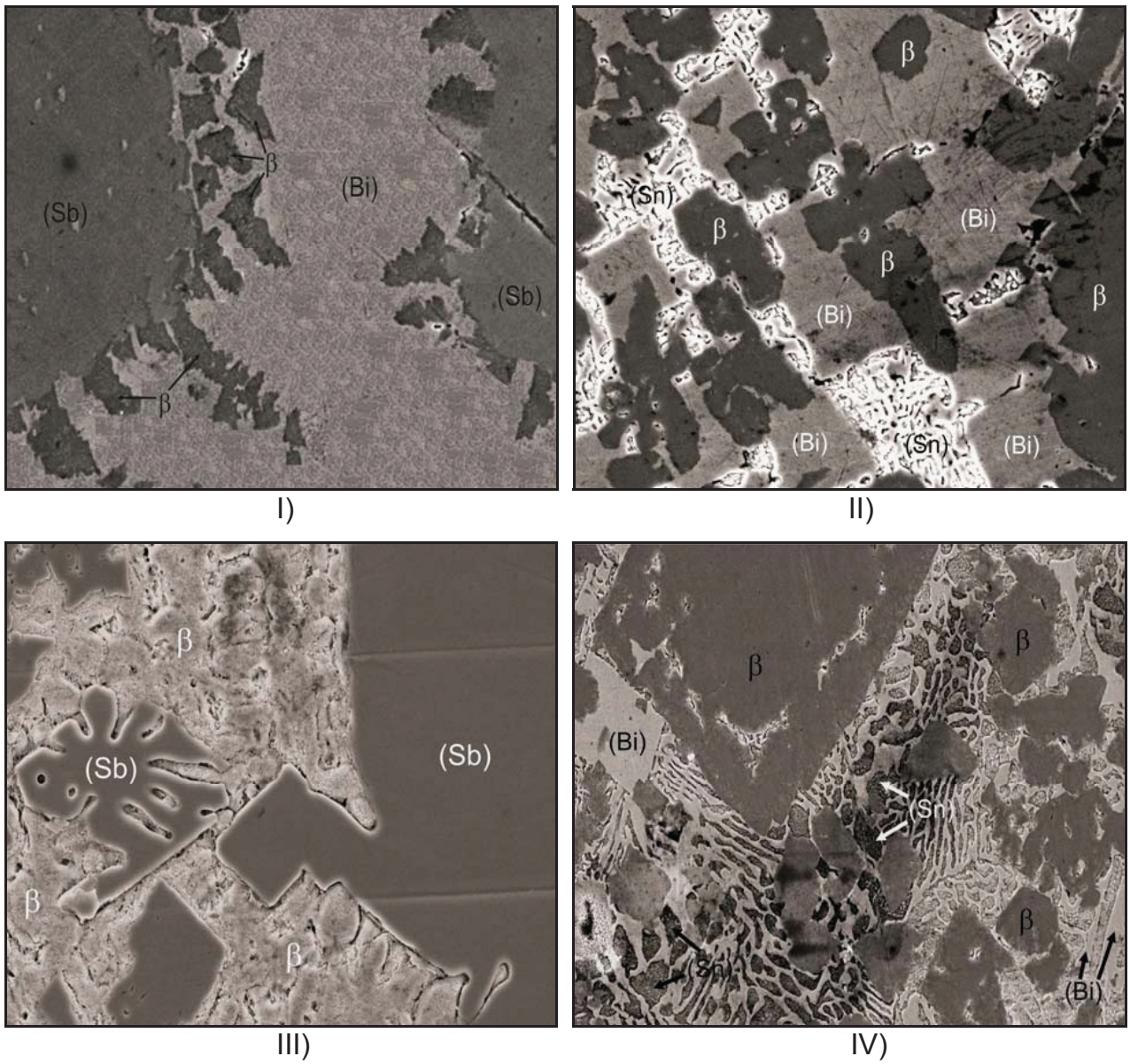

Figure 6. SEM micrographs illustrating microstructures of investigated alloys.

SEM images of the microstructures of the selected alloys with corresponding composition of the present phases determined by EDS point analysis are presented in Figure 6. Chemical compositions of all four investigated samples, phase compositions as well as calculated and experimentally determined compositions of the present phases are given in Table 3.

Experimentally obtained compositions, presented on Figure 6 and in Table 3. are in a good agreement with calculated compositions, however they differ considerably from the literature data.

Compositions of the alloys analyzed using light microscopy are given in Table 4. The investigated samples were prepared by conventional metallographic method

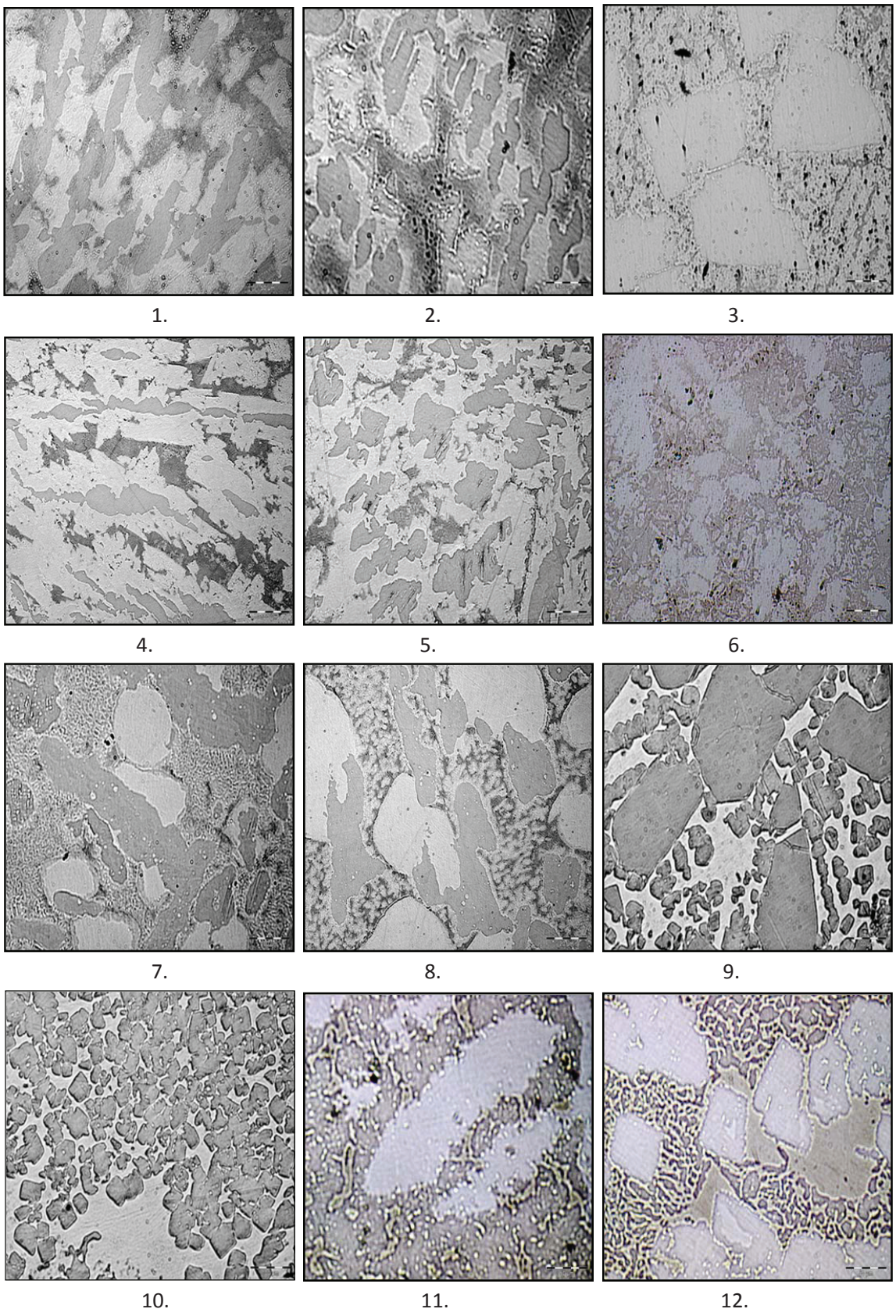

Figure 7. Microstructures of the alloys of ternary Bi-Sb-Sn system.

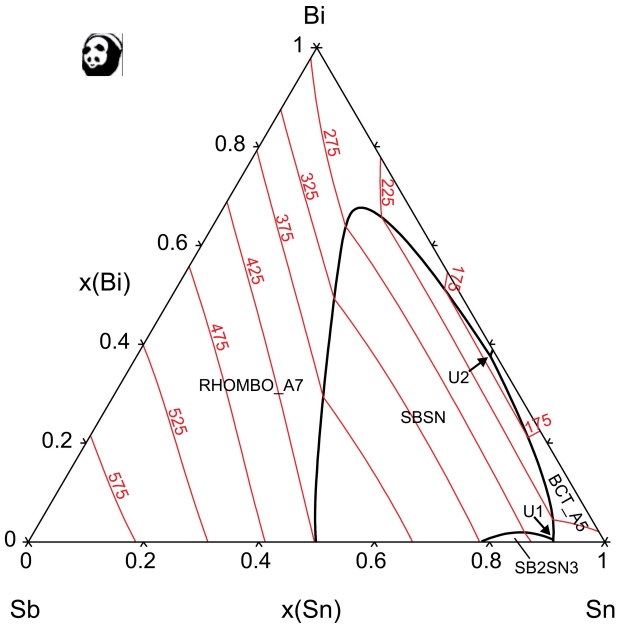

Figure 8. Liquidus surface projection of the ternary Bi-Sb-Sn system.

without etching. Obtained metallographic images of the investigated alloys are presented in Figure 7.

Alloys for which microstructural analysis has been carried out are marked on the isothermal section of ternary Bi-Sb-Sn system at 298 K presented on Figure 5. Alloy samples 1, 2, 7, 8 and 12 are from three-phase region ((Sn) + (Bi) + β) and within the presented microstructures three phases can be observed. Three-phase alloys are alloy samples 4, 5, and 9 as well. On the other side, alloy samples 3, 6, 10 and 11 belong to the two-phase region, which is well illustrated by the presented microstructures.

3.4 Liquidus Surface Projection

Calculated liquidus surface projection is presented on Figure 8.

On Figure 8, four primary crystallization fields can be observed: RHOMBO_A7, SBSN, SB2SN3 and BCT_A5. In the ternary Bi-Sb-Sn system two invariant reactions of U-type take place which represent liquidus transition reactions ($L+\alpha \rightarrow \beta+\gamma$). This is consistent with the previous study of Ghosh et al. [2].

Invariant reactions, reaction temperatures and type of the reaction are given in Table 5.

4 Conclusion

Brinell hardness and electrical conductivity were experimentally determined for the alloys from BiSn-Sb vertical section and all three vertical sections of ternary Bi-Sb-Sn system, respectively. Based on experimentally determined electrical conductivities of the alloys within the three quasi binary sections, isolines of electrical conductivity of ternary Bi-Sb-Sn system have been calculated by application of regression model. Using CALPHAD method, the isothermal section at 298 K has been calculated and compared to literature data. Microstructural analysis of the selected alloys shows good correspondence of the observed phases with the calculated number of phases within the isothermal section. Calculated liquidus surfaces were found to have four fields of primary crystallization and two invariant reactions which take place in this system.

Acknowledgments

The financial support of the Ministry of Education and Science of the Republic of Serbia under the Project ON 172037 is acknowledged. The results of this paper are also in the frame of the project COST MP0602. Calculations were performed using Pandat 8.1 software.

References

[1] R. Vogel, U. Apel, *Z. Metallkd.*, **44** (1953), 323–324.

[2] G. Ghosh, M. Loomans, M. E. Fine, *Journal of Electronic Materials*, **23** (7) (1994), 619–625.

[3] D. Manasijevic, J. Vrestal, D. Minic, A. Kroupa, D. Zivkovic, Z. Zivkovic, *Journal of Alloys and Compounds*, **438** (2007), 150–157.

[4] A. T. Dinsdale, A. Kroupa, J. Vízdal, J. Vrestal, A. Watson and A. Zemanova, COST531 Database for Lead-free Solders, Ver. 2.0, (2006) (unpublished research).

[5] N. Saunders and A. P. Miodownik, *CALPHAD (A Comprehensive Guide)*, Elsevier, London, (1998).

[6] I. Katayama, D. Zivkovic, D. Manasijevic, T. Tanaka, Z. Zivkovic, H. Yamashita, *Netsu Sokutei*, **32** (1) (2005), 40–44.

[7] A. T. Dinsdale, A. Watson, A. Kroupa, J. Vrestal, A. Zemanova and J. Vizdal (Editors), *COSTAction 531–Atlas of Phase Diagrams for Lead-free Solders*, Vol. 1, Brno, Czech Republic, (2008).

[8] M. Kolarevic, M. Rajovic, M. Bjelic, *Ternarni graf i njegova primena u regresionoj analizi*, IMK 14 OKTOBAR, **3–4** (22–23) (2005), 113–122.